Blight, Other Endothia *Diseases and the Genus* Endothia (APS Press, St. Paul, MN, 1986), pp. 1–53.
14. C. S. Hodges, *Myocologia* **72**, 542 (1980).
15. D. N. Appel and R. J. Stipes, *Plant Dis.* **68**, 851 (1984).
16. All five hypovirus-transfected fungal species were found to convert virus-free strains of the same species efficiently after anastomosis, as described (*6*). No cytoplasmic virus transmission was observed from transfected *C. parasitica* to other fungal species and vice versa.
17. B. I. Hillman, R. Shapira, D. L. Nuss, *Phytopathology* **80**, 950 (1990).
18. G. H. Choi and D. L. Nuss, *EMBO J.* 11, 473 (1992).
19. M. G. Craven, D. M. Pawlyk, G. H. Choi, D. L. Nuss, *J. Virol.* **67**, 6513 (1993).
20. T. G. Larson, G. H. Choi, D. L. Nuss, *EMBO J.* 11, 4539 (1992).
21. A. C. L. Churchill, L. M. Ciufetti, D. R. Hansen, H. D. Van Etten, N. K. Van Alfen, *Curr. Genet.* **17**, 25 (1991).
22. Plasmid pLDST used as a template for cell-free synthesis of the viral coding strand transcript contained a full-length cDNA copy of CHV1-713 L-dsRNA (*6*) flanked at the 5′ terminus by a bacteriophage T7 promoter sequence (TAATACGACTCACTATAG) and at the 3′ terminus by 22 adenosine residues, corresponding to the natural heterogenous polyadenylate tail found in L-dsRNA (*8*), followed by an Spe I restriction site. Thus, the synthetic transcript generated from Spe I linearized pLDST contained a nonviral G residue at the 5′ terminus and 22 adenosine residues followed by the vector sequence CUAG at the 3′ terminus. Cell-free transcription was performed with Riboprobe transcription reagents (Promega, Madison, WI) according to the manufacturer's instructions. Where indicated, reactions were treated with 3 units of RQ1-DNase or 0.3 unit of ribonuclease A for 20 min at 37°C. All reactions were extracted with phenol:chloroform, and nucleic acids were recovered by ethanol precipitation. Fungal spheroplasts (2×10^7 per milliliter) (*21*) in 100 μl of 1 M sorbitol were transfected with nucleic acid preparations (in 20 μl of H_2O containing 200 units of RNasin) by electroporation at 1.5 kV, 200 ohms, and 25 μF. The spheroplast suspensions were diluted with 750 μl of ice-cold 1 M sorbitol and incubated on ice for 5 to 10 min. Aliquots (200 μl) were then placed in the center of 10-cm petri dishes, surrounded by 20 ml of regeneration medium (*21*), gently mixed, and incubated at 25°C. Mycelial plugs were transferred from the edge of the regenerated colony to potato dextrose agar. Because hyphal strands regenerated from spheroplasts fuse with neighboring strands, replicating hypovirus RNA from transfected spheroplast can spread throughout the colony. Consequently, virus-infected mycelia can be readily obtained even at low transfection efficiencies without the need for a selectable marker.
23. Virulence assays were performed for uninfected and hypovirus-infected *E. gyrosa* on dormant pin oak and red oak stems as described (*24*). Thirty-five days after inoculation, bark was removed around lesions and the extent of the necrotic tissue was measured. Data are presented as the mean lesion area (in square centimeters) on the basis of four inoculations each of uninfected *E. gyrosa* and hypovirus-infected *E. gyrosa* per stem. Differences between lesion formation by virus-free and virus-containing fungal strains were highly significant for both host tree stems as indicated by the *t* values listed. The *E. gyrosa* species was chosen for the virulence assay because the natural plant hosts were readily available, it is a serious pathogen of stressed pin oak in urban settings (*15*), and it is classified in a different taxanomic family from members of the genus *Cryphonectria* (*11*).
24. R. A. Jaynes and J. E. Elliston, *Phytopathology* **70**, 453 (1980).
25. We thank S. Anagnostakis for providing fungal strains and advice on fungal taxonomy and M. Double and W. MacDonald for providing plant host material for virulence assays.

4 March 1994; accepted 28 April 1994

Recovery of Visual Response of Injured Adult Rat Optic Nerves Treated with Transglutaminase

Shoshana Eitan, Arieh Solomon, Vered Lavie, Eti Yoles, David L. Hirschberg, Michael Belkin, Michal Schwartz*

Failure of axons of the central nervous system in adult mammals to regenerate spontaneously after injury is attributed in part to inhibitory molecules associated with oligodendrocytes. Regeneration of central nervous system axons in fish is correlated with the presence of a transglutaminase. This enzyme dimerizes interleukin-2, and the product is cytotoxic to oligodendrocytes in vitro. Application of this nerve-derived transglutaminase to rat optic nerves, in which the injury had caused the loss of visual evoked potential response to light, promoted the recovery of that response within 6 weeks after injury. Transmission electron microscopy analysis revealed the concomitant appearance of axons in the distal stump of the optic nerve.

Nerves of the adult mammalian central nervous system (CNS) do not regenerate successfully after axonal injury. Spontaneous growth of injured axons does occur, but ceases after a few hundred micrometers, without traversing the injury site and without elongating into the distal stump (*1–4*). The failure to regenerate has been attributed to the inhospitable nature of the axon's local environment (*5–7*). One of the components of this environment, myelin-associated molecules produced by mature oligodendrocytes, inhibits axonal growth (*6, 8*). Unlike mammals, fish CNS spontaneously regenerates its injured axons. We recently identified in regenerating fish optic nerves an interleukin-2 (IL-2)–like compound, which has an apparent molecular weight twice that of Il-2 and is cytotoxic to oligodendrocytes in vitro (*9*). From the regenerating fish optic nerves we purified a nerve-derived transglutaminase (TG_N), capable of dimerizing IL-2 and making it cytotoxic to oligodendrocytes (*10*) through an apoptotic mechanism (*11*). These results, taken together with observations that the nerve preparation (regenerating fish optic nerve) from which TG_N is purified induces axonal growth in mammalian CNS in vivo (*12*) and that oligodendrocytes inhibit nerve regeneration in vitro (*6*), suggested to us that dimerization of IL-2 after injury may be an effective way to facilitate nerve regeneration. In addition, because the enzyme belongs to the family of transglutaminases, known to participate in tissue healing processes, it was anticipated that the enzyme might have additional activities beneficial to nerve regeneration. Here we examined this possibility by injecting the enzyme locally into injured optic nerves of adult rats. The nerves were then analyzed electrophysiologically in terms of recovery of the visual evoked potential (VEP) response to light, previously shown to be a reliable measure of the integrity of the visual

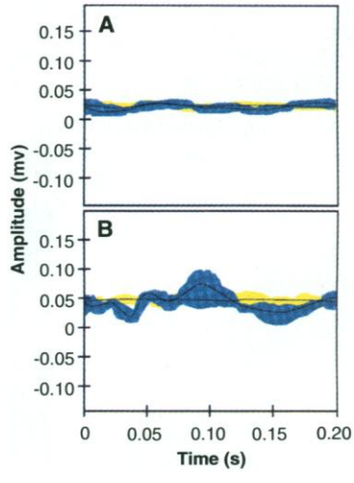

Fig. 1. Recordings of VEP response from a TG_N-treated injured nerve 1 week after injury. Nerves were injured and treated as described (*14*) and the VEP response was recorded (*15*). (**A**) Negative VEP response recorded from the left (injured) eye, while the right (uninjured) eye was covered during recording. (**B**) Positive VEP response recorded from the same animal while both eyes were open. Values are means obtained from three recordings (each involving 60 light flashes) (black line) ± SE (blue area). The baseline recording (black line) ± SE (yellow area) was made in the dark.

S. Eitan, V. Lavie, E. Yoles, D. L. Hirschberg, M. Schwartz, Department of Neurobiology, The Weismann Institute of Science, 76100 Rehovot, Israel.
A. Solomon and M. Belkin, Goldschleger Eye Research Institute, Sackler Faculty of Medicine, Tel Aviv University, Sheba Medical Center, Tel Hashomer, Israel.

*To whom correspondence should be addressed.

system from the retina to the cortex (*13*), and morphologically in terms of the presence of growing axons, assessed by transmission electron microscopy.

In the first experiment, 27 adult Sprague-Dawley rats were anesthetized and their left optic nerves were exposed and completely transected. Through an opening in the dura a dissecting needle was introduced and a buffer solution with or without TG_N was applied (*14*). Six weeks later the VEP response of the injured left optic nerve was recorded after implantation of two electrodes in the cerebral cortex of each animal (*15*). Surgical procedures, treatments, and recordings were done according to a double-blind protocol. The VEP response was positive in 14 of the 16 TG_N-treated animals and in 2 of the 11 control animals. The significant difference ($P < 0.0002$ compared by two binomial proportions) between the two groups appeared to preclude spontaneous recovery and suggested that treatment with TG_N was responsible for the observed response. The positive response observed in two control animals was probably due to some axons that had escaped injury. This was confirmed by electron microscopy (EM) analysis (*16*), which showed that an area within the lesioned nerve was apparently undamaged and contained normal-looking, myelinated axons.

To identify and exclude any rats exhibiting such postinjury residual activity, we carried out similar experiments, but implanted the electrodes and obtained the first recording of the VEP response (*15*) prior to the optic nerve injury. One week after injury the VEP response of the left eye was again recorded, while the right eye was covered by black tape to avoid the possibility of a response originating from it. In about 90% of the animals (22/25) the VEP response was negative (Fig. 1A). To confirm that the negative VEP response of the left eye recorded 1 week after injury was due to loss of activity in the nerve and was not a consequence of damage to the cortex caused by electrode implantation, recordings were also obtained while both eyes were open. As expected, we observed a small VEP response presumably resulting

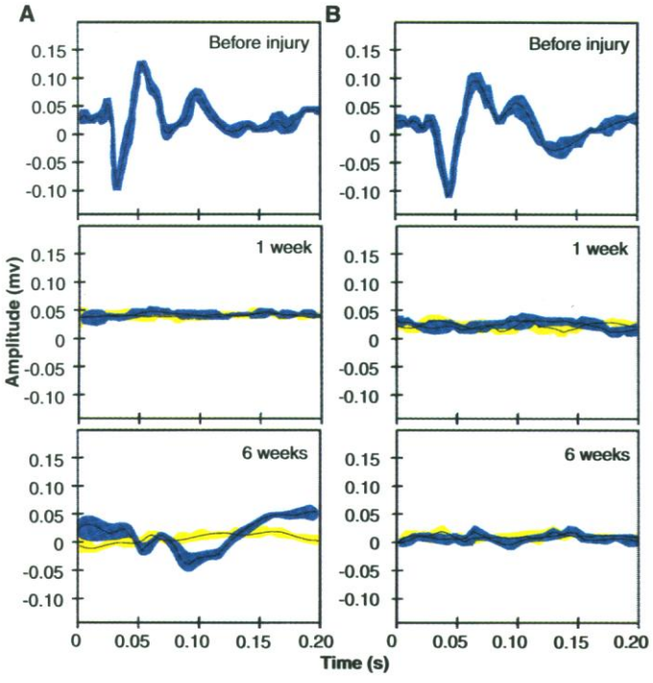

Fig. 2. Recovery of VEP response after injury. Nerves were injured and treated as described (*14*), and the VEP response was recorded (*15*). (**A**) Recording from a TG_N-treated animal before injury and 1 and 6 weeks after injury. Note that recovery is manifested by small peaks, all with longer latencies than those in the uninjured nerve. (**B**) Recording from a buffer-treated control injured animal before injury and 1 and 6 weeks after injury. Values are means obtained from three recordings (each involving 60 light flashes) (black line) ± SE (blue area). The baseline recording (black line) ± SE (yellow area) was made in the dark.

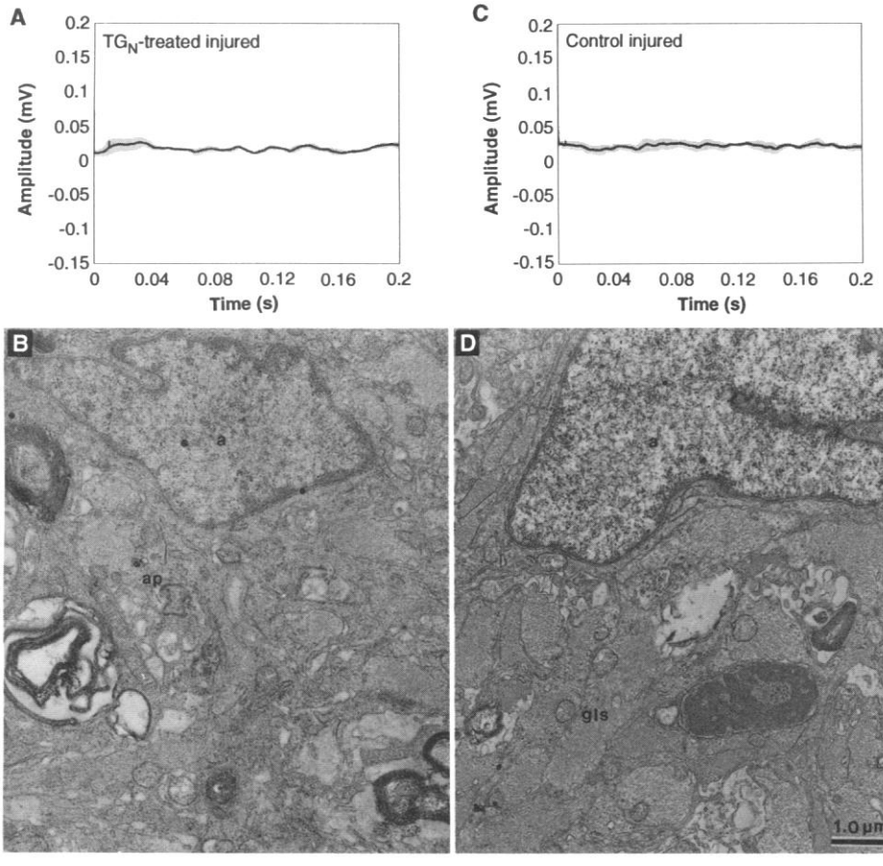

Fig. 3. Absence of spared viable axons at the site of injury in TG_N-treated and in buffer-treated control injured nerves, excised 2 weeks after injury. Nerves were injured and treated as described (*14*). Electrode implantation and recordings were carried out as described (*15*). The last VEP recording was carried out 2 weeks after the injury, and the nerves were then excised and processed for EM analysis (*16*). Ultrathin sections taken from the site of the injury were systematically analyzed. (**A**) Negative VEP responses of TG_N-treated animals. (**C**) Negative VEP responses of buffer-treated animals. Micrographs taken from the site of injury of TG_N-treated (**B**) and buffer-treated (**D**) nerves show a glial scar (gls) composed of astrocytes and their compactly packed processes (ap); in both preparations some myelin debris is also seen. Note the absence of viable myelinated axons at the site of injury in both preparations, indicating that the lesion was complete.

from the few fibers extending from the right eye to the right cortex (Fig. 1B). Only animals with no VEP response 1 week after injury were used in subsequent follow-up experiments. When the VEP response was recorded in these animals 6 weeks after injury, it was positive in 7 of the 10 TG_N-treated rats (Fig. 2A), but negative in all 12 control animals (Fig. 2B). Baseline recordings obtained in the dark were negative, confirming that the observed responses were evoked by light. The shift in latency of the response peaks of the TG_N-treated animals suggested the presence of unmyelinated or thinly myelinated axons in the TG_N-treated injured nerves (Table 1).

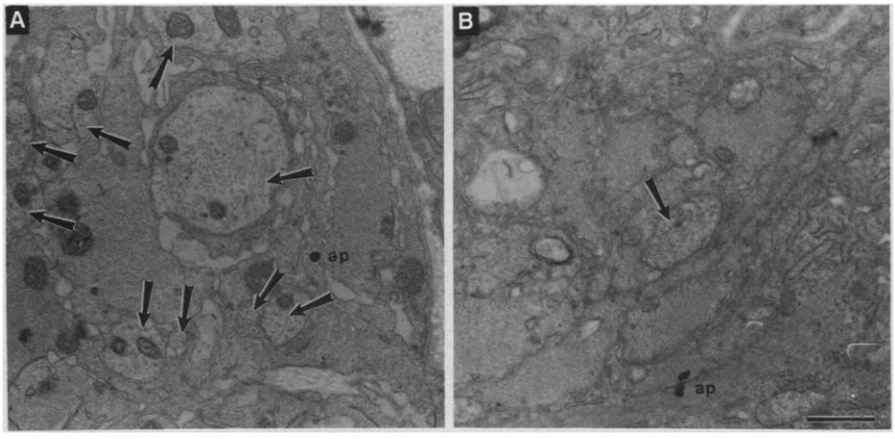

Fig. 4. Newly growing axons in TG_N-treated nerves 2 weeks after injury. The nerves shown in Fig. 3 were examined for the presence of unmyelinated axons at the site of the injury, both proximally and distally to it. These micrographs are of TG_N-treated nerves. Abundant unmyelinated axons (arrows) are seen embedded in astrocytic processes (ap) at the edge of the proximal stump and at the site of the injury (**A**), and a few (arrow) can be seen on the distal edge of the injury site and even penetrating the distal stump (**B**).

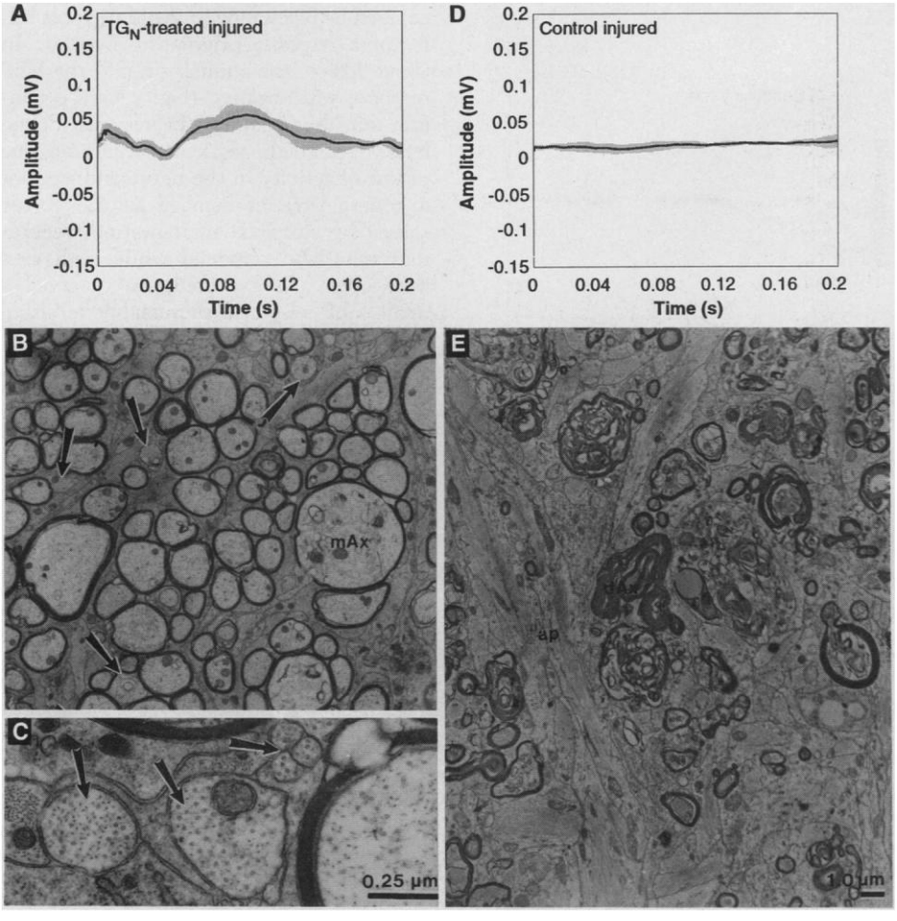

The electrophysiological measurements were accompanied by morphological analyses (*16*) with the same experimental paradigm. Two weeks after injury we analyzed four TG_N-treated injured animals and four control injured animals that had shown no VEP response 1 week after injury. No spared (normal-looking myelinated) axons could be detected at the injury site in either buffer-treated control (Fig. 3D) or TG_N-treated (Fig. 3B) nerves. In both preparations degenerating axons and some debris were observed. However, in the TG_N-treated nerves, an abundance of unmyelinated nerve fibers resembling newly growing axons were embedded in astrocytes at the proximal edge of the injured nerve (Fig. 4A), and a few could also be seen at the site of the injury and even penetrating the distal stump (Fig. 4B). In buffer-treated injured nerves, a few unmyelinated axons were seen at the proximal nerve stump and none at the injury site. Six to 8 weeks after injury, we analyzed four TG_N-treated injured animals and two control injured animals that had shown no VEP response 1 week after injury. Proceeding distally from the site of injury, cross sections of the nerves were taken at 1-mm intervals and analyzed. In the buffer-treated nerves no viable fibers could be detected in any of the sections (Fig. 5E). In the enzyme-treated nerves, however, at the same time as positive VEP responses were recorded (Fig. 5A), nerve fibers resembling newly growing axons were seen throughout the entire length of the nerve (Fig. 5, B and C). The fibers were either unmyelinated or thinly myelinated and were far less densely packed than in uninjured nerves, becoming

Fig. 5. Correlation between physiological and morphological observations 6 to 8 weeks after injury. After recording of the VEP response 8 weeks after injury, the left optic nerves from a representative buffer-treated and TG_N-treated animal were excised and processed for transmission electron microscopy analysis, as described (*12*). (**A** and **D**) VEP responses 6 weeks after injury in TG_N-treated and buffer-treated animals, respectively. (**B** and **C**) Representative electron micrographs taken from an area 1 mm distal to the injury site of the TG_N-treated injured nerve. (**E**) Representative electron micrograph from an area 1 mm distal to the injury site in the buffer-treated nerve; mAx, myelinated axon; dAx, degenerating axon. Arrows point to unmyelinated axons. Note that in the control nerve the entire area is occupied by degenerating axons, myelin debris, and astrocytic processes (ap). In the TG_N-treated nerve the compartment containing viable nerve fibers is almost free of degenerative debris.

less densely packed with increasing distance from the injury site. They were embedded in astrocytes and formed a compartment almost free of degenerative tissue and myelin debris (Fig. 5, B and C). The rest of the section, like the entire corresponding sections from buffer-treated injured nerves, showed densely packed astrocytes (glial scar), degenerating axons, and myelin debris (Fig. 5E). Two nerves from TG_N-treated animals were further analyzed quantitatively along their length starting 1 mm proximal to the injury site and proceeding distally. The total number of nerve fibers in each section (Fig. 6) was counted on a montage incorporating all the micrographs corresponding to that section. The number of fibers, all of which appeared in one compartment, decreased with increasing distance from the injury site, suggesting that at least some of the fibers were regrowing axons: If they were axons that had escaped primary injury or that had not yet degenerated, their numbers would have been equal throughout the nerve's length or increased with distance, respectively.

The results of this study demonstrate postinjury recovery of physiological activity after treatment with TG_N. The following findings provide evidence that the observed recovery may be due to regenerative growth of axons: (i) Loss of activity, as assessed by electrophysiological measurements 1 week after injury, indicated that the injury was complete, and this was confirmed morphologically by the absence of viable axons at the injury site 2 weeks after injury; (ii) VEP response was recovered after 6 to 8 weeks in TG_N-treated but not in buffer-treated injured nerves; (iii) the latency of the recovered VEP response was longer than that of the VEP response in uninjured nerves; (iv) 6 to 8 weeks after injury, thinly myelinated and unmyelinated axons appeared distally to the site of lesion in the TG_N-treated but not in the buffer-treated nerves; and (v) these axons decreased in number with increasing distance from the injury site.

The apparent participation of TG_N, a member of the transglutaminase family, in nerve healing suggests that processes associated with the healing of other tissues also apply to the nervous system. Although the nervous system does not normally regenerate in response to trauma, it apparently has not lost the potential to do so and may regenerate if provided with enzymes and factors associated with the body's normal healing mechanisms. We suggest that TG_N dimerizes IL-2 in vivo as it does in vitro, leading to early postinjury elimination of mature oligodendrocytes, at least in the immediate vicinity of the injury site. Support for this proposed mechanism comes from our observation that along the nerve, the compartment of apparently newly growing axons was almost free of myelin debris and degenerating axons (Fig. 5, B and C). The regenerative growth observed after application of antibodies directed against inhibitors of oligodendrocytes, as demonstrated by Schnell and Schwab (*17*), is in line with this notion.

Regenerative growth of axons in the degenerative environment of the adult CNS presumably depends on synchrony between two interdependent processes, axonal regrowth and environmental acquisition of growth-supportive properties. It seems likely that in a nonregenerating system these processes might occur spontaneously but nonsynchronously, and that the lack of synchrony might be a reason for the failure of axons to grow (*18*). That in the present study a single injection of the enzyme at the injury site was apparently enough to cause the complete growth of axons suggests that the growth of axons and the elimination, at least in part, of growth inhibitors might be brought into synchrony, possibly by an earlier than normal death of oligodendrocytes in response to treatment with TG_N. The applied TG_N might also contribute locally to the stabilization of matrix proteins, a known activity of transglutaminases (*19*, *20*). A single application would also suffice to produce these results if the enzyme enters the growth cones, where it might act as a safeguard (*21*) helping to protect the growing axons from collapse induced either by the oligodendrocyte-mediated inhibitory effect (*22*) or directly by local Ca^{2+} elevation.

Table 1. Characteristics of VEP response in intact optic nerves and in TG_N-treated and buffer-treated optic nerves 6 weeks after injury.

Group	Latency* (s)	Amplitude† (mV)	Animals (no.)
TG_N-treated injured nerves	0.0620 ± 0.0045	0.036 ± 0.003	10‡
Buffer-treated injured nerves	0	0	12
Intact nerves	0.0400 ± 0.0014	0.132 ± 0.009	12

*df = 1, F = 34.018, P = 0.0001; one-way analysis of variance. †df = 1, F = 93.101, P = 0.0001. Comparison revealed significance at 95%. ‡Animals (three) with no VEP response 6 weeks after injury were not included in the calculations of latency and amplitude.

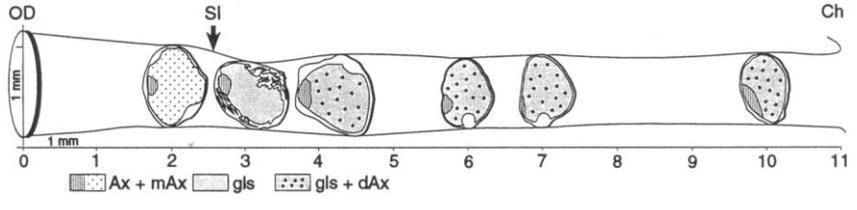

Fig. 6. Schematic reconstruction of an enzyme-treated injured nerve. The compartment of regenerative growth (Ax + mAx) under the dura is continuous throughout the entire length of the nerve. Sections were taken at 1-mm intervals along the nerve. Each section was photographed in its entirety at a magnification of ×5600, a montage was constructed, and the total number of viable axons was counted. In the nerve depicted in the figure the number of viable axons (at increasing distances from the globe) was as follows: 1500 (2 mm), 782 (3 mm), 780 (4 mm), 570 (6 mm), 606 (7 mm), and 400 (10 mm). OD, optic disk; SI, site of injury; Ch, optic chiasm; gls, glial scar; dAx, degenerating axons.

REFERENCES AND NOTES

1. P. M. Richardson, V. M. K. Isaa, S. Shemie, *J. Neurocytol.* **11**, 949 (1982).
2. J. A. Kiernan, *Biol. Listy* **54**, 155 (1979).
3. S. Ramón y Cajal, *Degeneration and Regeneration of the Nervous System*, R. M. May, Trans. (Hafner, New York, 1954), vol. 1.
4. B. Grafstein and N. A. Ingoglia, *Exp. Neurol.* **76**, 318 (1982).
5. K. F. So and A. J. Aguayo, *Brain Res.* **328**, 349 (1985); S. A. Keirstead *et al.*, *Science* **246**, 255 (1990); A. J. Aguayo *et al.*, *Exp. Biol.* **153**, 199 (1990).
6. M. E. Schwab and H. Thoenen, *J. Neurosci.* **5**, 2415 (1985); M. E. Schwab and P. Caroni, *ibid.* **8**, 2381 (1988).
7. M. Schwartz *et al.*, *Science* **228**, 600 (1985).
8. T. Sivron, M. E. Schwab, M. Schwartz, *J. Comp. Neurol.* **343**, 237 (1994).
9. S. Eitan *et al.*, *Proc. Natl. Acad. Sci. U.S.A.* **89**, 5442 (1992).
10. S. Eitan and M. Schwartz, *Science* **261**, 106 (1993).
11. O. Eizenberg, A. Elman-Faber, M. Schwartz, unpublished results.
12. V. Lavie *et al.*, *J. Comp. Neurol.* **298**, 293 (1990).
13. L. J. Dorfman *et al.*, *Neurology* **37**, 123 (1987).
14. The left optic nerve was exposed through a small opening in the meninges. The nerve fibers were completely transected 2 to 3 mm from the globe, without damage to the nerve vasculature and with minimal damage to the meninges, by the use of a specially designed glass dissector with a 200-μm tip and a smooth blunt edge. To transect the nerve, the tip of the dissector was moved horizontally from right to left while being introduced slowly throughout the depth of the nerve until the whole width was traversed. The meninges surrounding the nerve were kept intact, except for the opening through which the dissector was inserted. Buffer solution (2 μl), without or with TG_N [~15×10^{-6} U; measured by incorporation of [^{3}H]putrescine into *N,N*-dimethylcasein using guinea pig liver transglutimase (Sigma) as a standard], was introduced by way of a glass pipette through the meningeal opening. This was followed by daily He-Ne laser irradiation (632 nm, 10 mW, 5 min) for six consecutive days, which was found to

attenuate the postinjury process of degeneration [E. Assia, M. Rosner, M. Belkin, A. Solomon, M. Schwartz, *Brain Res.* **476**, 205 (1988)]. The combined treatment of low-energy laser irradiation with local injection of soluble substances into injured optic nerves promotes axonal growth in the rabbit optic nerve model (*12*).

15. Rats were deeply anesthetized and placed in a small stereotaxic instrument. In each animal two holes were drilled in the skull, through which two electrodes were implanted, while the dura were kept intact to minimize cortical damage. The electrodes were gold contact pins (Wire-Pro) soldered to screws, which were screwed into the holes and cemented to the skull with acrylic cement. The electrode inserted through the hole drilled in the nasal bone was used as a reference point. The second hole was in area OC1, with coordinates bregma 8 mm and lateral 3 mm. The field potential evoked by the left eye, recorded in the right visual cortex before and after injury, was evoked by stroboscopic light stimulation after implantation of the electrodes. The stroboscopic light had the following characteristics: xenon flash tube (4 W/s, 1- to 2-ms duration, 0.3 Hz) amplified 1000 times (AM Systems, microelectrode AC amplifier, model 1800) and digitized (12 bits, 5000 samples per second) (National Instruments, board NB-MIO16-9 and LabView 2.2.1 data acquisition and analysis software). Unless otherwise indicated, the right eye was covered by black tape during recording of the VEP response to avoid the possibility of a VEP response originating from it.
16. Rat optic nerves were excised and fixed by immersion in 1% paraformaldehyde and 2% glutaraldehyde in 0.1 M cacodylate buffer (pH 7.4) containing 2.5 mM $CaCl_2$. The nerves were cut with a razor blade into segments 1 mm long, which were postfixed for 60 min with 1% osmium tetroxide containing 1% potassium ferricyanide in cacodylate buffer, stained en bloc in uranyl acetate (2% in water) for 30 min, and dehydrated by immersion in increasing concentrations of ethanol and then in propylene oxide. Nerve segments were infiltrated with Polybed (Polysciences, Warrington, PA) and cured for 3 days at 60°C. Ultrathin sections were placed on 300-mesh or on formvar-coated one-slot copper grids, stained with lead citrate and saturated uranyl acetate, and examined with a Philips 410 electron microscope. Axons were classified as myelinated if their axoplasm was lucent, their microtubules and neurofilaments were aligned, and their myelin was well preserved. Axons were classified as unmyelinated if they contained aligned microtubules and neurofilaments, lucent cytoplasm, and occasional vesicles.
17. L. Schnell and M. E. Schwab, *Nature* **343**, 269 (1990).
18. S. David *et al.*, *Neuron* **5**, 463 (1990).
19. J. E. Folk, *Annu. Rev. Biochem.* **49**, 517 (1980).
20. C. S. Greenberg, P. J. Birckbichler, R. H. Rice, *FASEB J.* **5**, 3071 (1991).
21. I. Facchiano *et al.*, *Trends Biochem. Sci.* **18**, 327 (1993).
22. C. E. Bandtlow *et al. Science* **259**, 80 (1993).
23. Supported by Farmitalia Carlo Erba, Italy. M.S. is the incumbent of the Maurice and Ilse Katz Professorial Chair in Neuroimmunology. The editorial assistance of S. Smith is acknowledged.

31 January 1994; accepted 6 May 1994

Silencers and Domains of Generalized Repression

Stephen Loo and Jasper Rine*

Gene expression can be affected by the chromosomal position of the gene. An example of this position effect is silencing of the *HML* and *HMR* mating-type loci of *Saccharomyces cerevisiae*. An in vitro assay revealed that silencing induced a transcription-independent general occlusion of the DNA at *HMR* from sequence-specific interactions of proteins with DNA. The minimum boundaries of the silenced chromatin structure were determined, as were the contributions of the E and I silencers to the size of the silenced domain. Examination of endonuclease-sensitive sites provided evidence that neither the integrity of the chromosomal duplex nor covalent linkage of the silencers to *HMR* was important for maintenance of the silenced structure in vitro.

The eukaryotic genome is arranged into functional domains that influence states of gene expression. Euchromatic regions are highly transcribed, whereas heterochromatic regions are not. Transcriptionally quiet regions are often close to chromosomal landmarks, such as centromeres and telomeres in *Drosophila melanogaster* (*1*, *2*), telomeres in *Saccharomyces cerevisiae* (*3*), and centromeres in mouse (*4*) and *Schizosaccharomyces pombe* (*5*). Genes transposed next to heterochromatin acquire a lower level of expression. The mechanisms by which these position effects operate are not gene specific and may represent a general inactivation of chromosomal segments.

An example of a position effect in *S. cerevisiae* is the transcriptional repression of genes at the mating-type loci *HML*α and *HMR***a**. This block to gene expression shares several characteristics with heterochromatic repression and has been named silencing. Mating-type in *S. cerevisiae* is determined by the information encoded at the *MAT* locus. The *MAT***a** and *MAT*α alleles encode the regulatory proteins that impart the **a** and α mating phenotypes of the haploid cell types and the nonmating, sporulation-proficient phenotypes of the **a**/α diploid (*6*). Most strains of *S. cerevisiae* also have copies of both the α and **a** genes at the transcriptionally repressed *HML*α and *HMR***a** loci. These copies of the α and **a** genes are not expressed unless they are transposed to the *MAT* locus during mating-type switching. Mating-type switching is catalyzed by HO endonuclease cleavage of *MAT*. HO endonuclease cannot cleave its recognition sequences at *HML*α or *HMR***a** (*7*); however, mutations that allow transcription of *HML*α and *HMR***a** at their native chromosomal locations also allow cleavage by HO endonuclease (*8*). Thus, *HML* and *HMR* contain all the sequences necessary for successful transcription, but their transcription is blocked by a combination of proteins and sites that mediate silencing.

Several proteins that are important for silencing have been identified by genetic criteria (*9*). Inactivation of *SIR2*, *SIR3*, or *SIR4* results in complete derepression of *HML* and *HMR*, as well as loss of the telomeric position effect, with few other phenotypes. Mutations in the NH_2-terminus of histone H4 also derepress *HML* and *HMR* (*10–13*). Additional insights into the role of chromatin structure have been obtained from the observations that *SIR2* overexpression results in hypoacetylation of histones (*14*), *SIR3* and histone H4 interact genetically (*11*), and a *SIR3* mutation affects the conformation of a histone H3 variant bound at *HMR* (*15*).

Sequence elements, known as silencers, flanking *HML* and *HMR* are required for repression. *HML* is flanked by the *HML*-E and *HML*-I silencers, and *HMR* is similarly flanked by *HMR*-E and *HMR*-I (*16–18*). The silencers are complex and resemble yeast autonomous replication sequence (ARS) elements, and several observations suggest a role for DNA replication in silencing (*16*, *19–23*). The arrangement of one silencer on each side of *HML* and *HMR* suggests that it is important that both sides of the region under control are flanked; however, in some contexts, single silencers are fully capable of repression (*18*, *24*).

We developed an in vitro assay that mimicked the dependence of the silenced region on both *SIR* function and the presence of the silencers. Isolated yeast nuclei were assayed with purified HO endonuclease to determine whether the DNA at the silent mating-type loci remained in a repressed state. Cleavage by the HO endonuclease in vivo occurs only at *MAT* in wild-type cells; however, in *sir* strains, *HML* and *HMR* are also cleaved by HO endonuclease, allowing mating-type switching at any of the three loci (*7*, *8*). *SIR*-dependent HO endonuclease cleavage was detected in isolated nuclei (Fig. 1A). In wild-type nuclei, only the *MAT* locus was cleaved by HO endonuclease. In contrast, both *MAT* and *HMR* were cleaved in nuclei from a *sir4* strain. Similar results were observed with nuclei from *sir2* and *sir3* strains and for the *HML* locus (see below). Furthermore, the amounts of *MAT* and *HMR* cleaved in nuclei from *sir* strains

Department of Molecular and Cell Biology, Division of Genetics, 401 Barker Hall, University of California at Berkeley, Berkeley, CA 94720, USA.

*To whom correspondence should be addressed.